Proceedings of the
Annual Stability Conference
Structural Stability Research Council
Louisville, Kentucky, April 1-4, 2025

Double-storey cold formed steel shear wall tests with integrated built-up uprights subject to monotonic load

Xinxin Liu[1], Mani Khezri[2], Kim Rasmussen [3]

Abstract
Steel-sheathed cold-formed steel shear walls (CFSSW) are commonly utilised in low-rise residential buildings and warehouses worldwide, designed to established specifications. Adapting CFSSW for mid-rise and high-rise structures subjected to substantial gravity and horizontal loads (wind or seismic) necessitates the use of built-up sections in framing the shear panels to enhance lateral strength and stiffness. This paper presents stage one of a shear wall test program involving 6 CFSSW specimens of double-storey configurations with various arrangements of built-up uprights comprising two or more screw-connected sections. The specimens are tested under monotonic loads. The program's objective is to assess the impact of using built-up members on overall shear stiffness and strength compared to traditional equally spaced single studs. Additionally, this paper discusses the influence of floor-to-floor connections on the lateral drift and in-plane rotation of double-storey shear walls. The test program also serves to validate the accuracy of future finite element models. The test setup, loading protocols, and experimental results are detailed in the paper.

1. Introduction
Steel-sheathed cold-formed steel shear walls (CFSSWs) are widely employed in low-rise buildings due to their efficiency, cost-effectiveness, and compliance with established design specifications. Over the past couple of decades, extensive experimental research has significantly enhanced understanding of their performance, and provided a database of over 700 shear wall tests, which has supported the development of design standards like AISI S240 and AISI S400 (Zhang et al. 2024). Informed by 27 studies such as those by Serrette et al. (1997), Boudreault (2005), and Santos (2018), tests revealed that steel sheet sheathing undergoes less sudden strength loss at the failure stage, compared to other sheathing material like oriented-strand board (OSB) (Serrette et al. 2006). Monotonic and cyclic tests on steel sheathing CFSSW of varying thicknesses and aspect ratios were also conducted by Yu (2010), revisiting the high aspect ratio reduction factor adopted in the AISI design standard. (Singh et al. 2020) investigated the performance of CFS in-line wall systems (i.e. gravity walls, shear walls and wall finishes along the same structural line) under seismic conditions. The tests demonstrated improved stiffness performance when wall finishes

[1]PhD student, The University of Sydney, <xinxin.liu@sydney.edu.au>
[2]Sinor Lecturer, The University of Sydney, <mani.khezri@sydney.edu.au>
[3]Professor, The University of Sydney, <kim.rasmussen@sydney.edu.au>

were added and a reduced stiffness due to structural asymmetry. Moreover, Peterman, Nakata, and Schafer (2014) characterised the hysteretic response of stud-to-sheathing connections, highlighting the influence of fastener spacing and sheathing type on shear capacity. These contributions, combined with advancements in computational modelling, such as those by Shamim, DaBreo, and Rogers (2013), have refined the design and analysis of CFS shear walls, ensuring safer and more efficient structures. However, the application of CFSSWs in mid-rise and high-rise structures is still limited due to increased demands for lateral strength and stiffness to withstand substantial gravity and lateral loads. Built-up sections have been proposed in recent studies as an innovative solution to enhance CFSSW performance for these applications. By connecting multiple components using fasteners, built-up sections may provide greater stiffness and strength compared to traditional equal-spaced single-section framing. Back-to-back built-up studs with centre-sheathed wall configuration were able to achieve shear strength up to 145.94 kN/m, described as the shear capacity per unit wall width (Brière 2018).

While extensive single-storey CFSSW tests have been conducted, simply extrapolating their results to multi-storey applications could be insufficient due to the ignorance of the contribution of floor-to-floor connections to overall structure integrity. Even with the assumption of rigid connections between floors, the features unique to multi-storey systems including dynamic response, load redistribution, and boundary effects cannot be fully replicated in single-storey setups. As such, the understanding of structural performance of shear wall system in mid-rise buildings remains limited. Double-storey shear wall tests presented in this paper aims to address this gap by including the inter-storey interactions, cumulative deformation effects, and the influence of floor-to-floor connections into the tests. The tests also allow for the evaluation of how innovative built-up configurations contribute to stability and stiffness under monotonic loads. This paper presents the first series of an experimental programme aimed at understanding the behaviour of CFSSWs in double-storey configurations. A total of six specimens, constructed as cold-formed steel screw-fastened (CFSSW) assemblies with double-storey configurations, were tested under monotonic loading conditions. The specimens had variations in built-up upright arrangements, sheet thicknesses, and fastener schedules. The study evaluates the impact of built-up members on shear stiffness and strength and investigates the role of floor-to-floor connections in lateral drift and in-plane rotation. The findings will inform computational models and design guidelines for mid-rise CFSSWs, advancing their application in multi-storey structures.

The structure of the paper is as follows. Section 2 describes the experimental program, detailing the test setup, specimen design, and test matrix. Section 3 presents the key observations and results, focusing on the effects of flooring configuration, built-up sections, and sheathing thickness. Section 4 concludes the paper by summarising the findings and discussing their implications for the design and optimisation of CFSSWs in mid-rise structures.

2. Experiment program

2.1 Test setup

The shear wall specimen is placed on the purpose-built rig (as per design drawing shown in Fig. 1(a)). The complete assembly of the test rig (Fig. 1(b)) is comprised of three components: (1) self-reactive frame and subframe for jack mount (Figs. 2 (a) and (b)), (2) out-of-plane support structure (Fig. 3), and (3) loading system (Fig. 4).

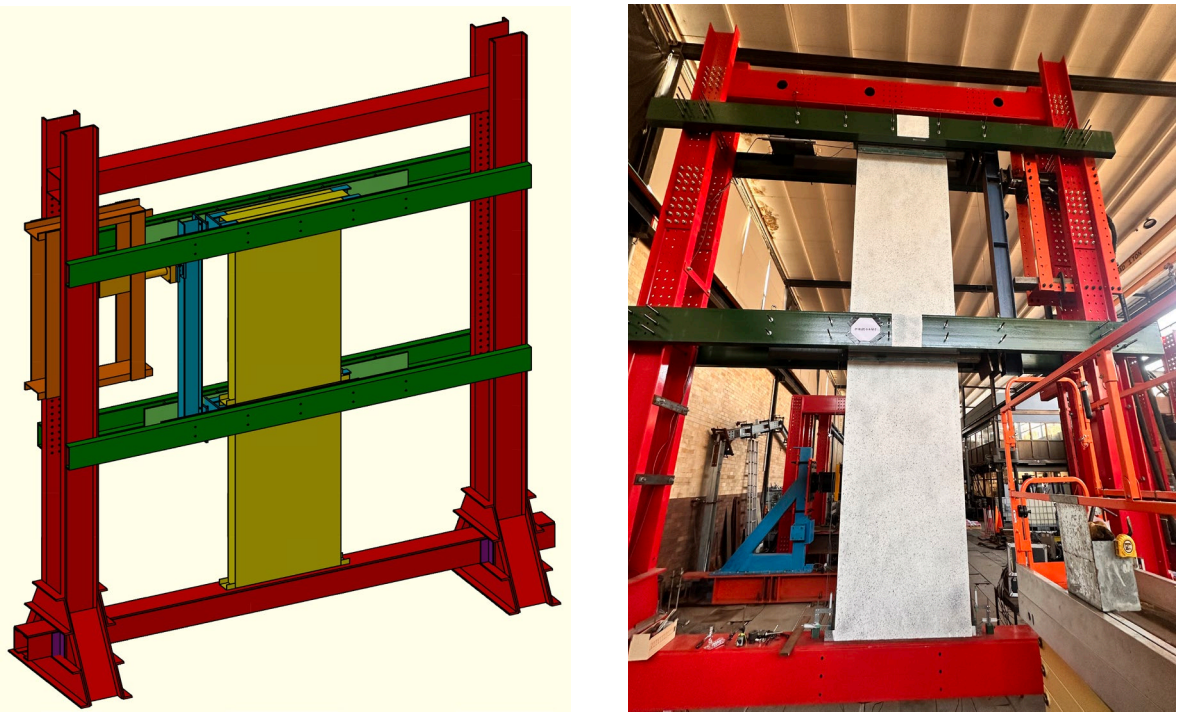

(a) 3D schematic drawing by Auto CAD (b) Assembled test rig

Fig. 1: Complete test rig setup with components grouped by colours

Referring to Fig. 2 (a), the shear wall specimen is placed and secured onto a 4.88m (wide) × 6.57m (high) self-equilibrating frame. The frame is connected to the lab strong floor beams for extra stability. Loads are applied to the specimen by a dual-glide hydraulic actuator with a maximum load capacity of 250kN. The actuator is bolted onto the mounting cage with angle brackets and then connected to the rig frame (as indicated in Fig. 2 (b)). The support system was designed to prevent any out-of-plane displacement or rotation at the inter-storey level, as shown in Fig. 3. Looking into the side elevation of the support structure (Fig. 3 (b)), threaded bars and 10 mm steel pads were welded onto a 3 m steel strip, functioning as an adjustable lateral restraint.

The loading mechanism (Fig. 4 (a)) adopted in this experiment takes the actuator load and divides it into 2 point loads by a 200UB29.8 spreader beam with a length of 2500mm. A total of 4 Parallel Flange Channels (PFC)s, two at each floor level on both sides of the shear wall are nested and bolted onto the rim tracks (Fig. 5(b)) through both flanges (Fig. 4 (b)). The load beams represent the floor system actions, transferring lateral loads onto the shear wall system in the real building structure. During tests, the webs of the loading beams will be in contact with the lateral restraints. Hence, to avoid any artificial friction forces being introduced to the system by the lateral restraint, 1 m long Teflon plates are attached to the webs of all four loading beams. The designed test rig allows various ratios of shear forces between the floors ($\varphi = F2/F1$) to be adopted, achieved by adjusting the location of the actuator-to-spreader beam connection, where $F1$ and $F2$ are the lateral forces applied at mid-height and the top of the shear wall, respectively. In choosing the load ratio (φ), study was conducted on ratios used in previous test programs. Broadly, for multi-storey shear wall tests, the load distribution can be classified into the following categories: loads applied exclusively at the top floor (Li et al. 2010; Mori et al. 2008; Reynolds et al. 2017), equal loads applied at each level (Driver et al. 1998; Shahnewaz, Dickof, and Tannert 2021), and customised

load ratios tailored to specific test objectives (Wang and Ye 2016). It is noted that not all tests referenced in this section were CFSSWs, but they are considered applicable for solely the purpose of designing the load ratio for multi-storey shear wall tests. In the present series of tests, the shear force transferred onto the shear panel at each level can be chosen according to the total number of storeys of the building the test represents. By equilibrium, for a given load ratio (φ), the load from the actuator shall be applied to the spreader beam at a location corresponding to $1/(1+\varphi)$ of the total distance between the two slotted scissor joints, measured from the top joint. A load ratio of five is chosen for the tests, representing the ratio of loads transferred onto the bottom two shear wall systems for a typical 7-storey mid-rise building.

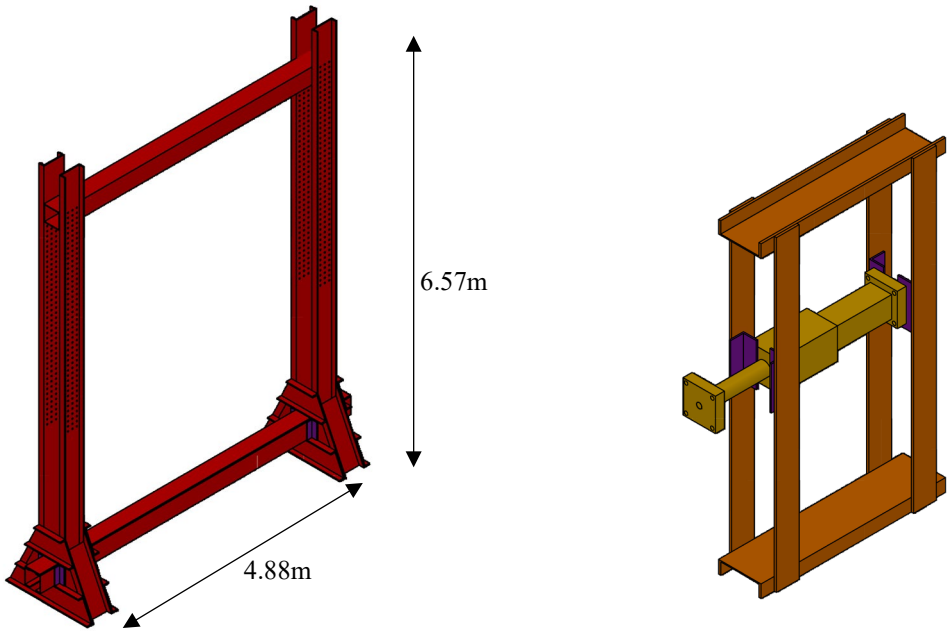

(a) Self-reactive frame 6.57m (H) × 4.88m (W) (b) Subframe securing jack onto the reactive frame

Fig. 2: 3D drawings of frame systems in the test rig

A scissor joint is used to connect the spreader beam and jack to ensure that no moment is exerted on the loading beams (as detailed in Fig. 4 (c)). A regular pin connection typically involves a single set of flat plates on one part, nesting on a plate on the other part, and joined through a pin. The scissor joint, on the other hand, consists of two sets of plates with a space in-between, creating a fork-like joint. This type of joint allows the load to be distributed across a wider surface area, reducing stress concentration on the connection. Moreover, the scissor joint provides better force alignment because the parallel plate setup ensures that the load is transferred symmetrically through the centreline of the pin, whereas regular pin connections may introduce slight misalignment due to off-centre force application, particularly for tests with high lateral loads or large displacements. Slotted scissor joints are adopted for the connection between the spreader beam and the loading beams, as illustrated in Fig. 4(c). The connector modifies a standard scissor joint by incorporating a slotted groove, which enables the free movement of the specimen along the groove, in addition to free rotation about the pin. This design eliminates any artificial vertical constraints imposed on the shear wall, thereby enabling the test to capture vertical movements (uplift) of the specimen between the floors.

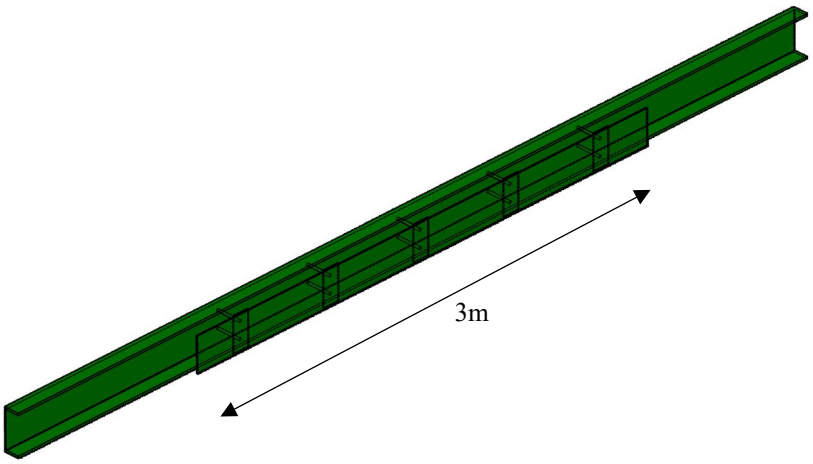

(a) 3D schematic drawing of lateral support on one side

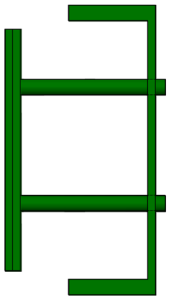

(b) Side view

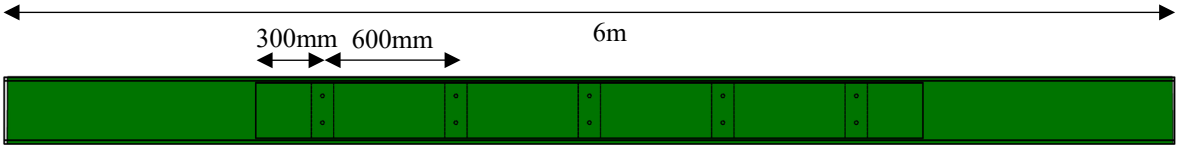

(c) Plan view

(d) Elevation view

Fig. 3: Out-of-plane support system drawings

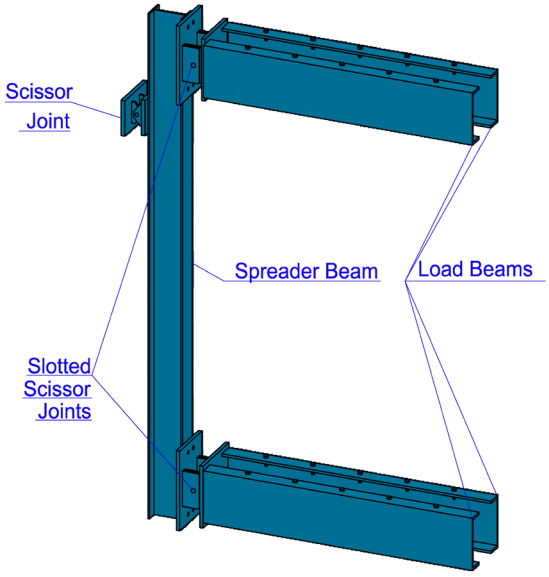

(a) 3D schematic drawing

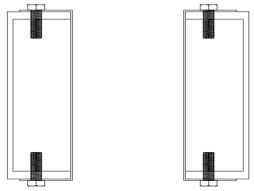

(b) Load beam to rim track connection

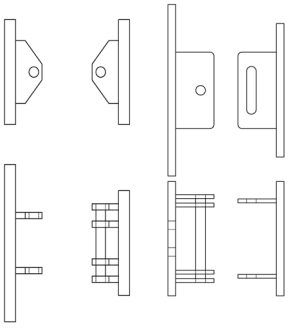

(c) Scissor joint and slotted scissor joint

Fig. 4: Loading mechanism with detailed breakdown of components

The standard loading protocol for static shear wall testing (American Society for Testing and Materials 1998), established by the American Society for Testing and Materials (ASTM) International, was adopted for this test program. An initial load equivalent to 10% of the estimated capacity was applied to the specimen at a constant displacement-controlled rate of 4 mm/min. The test was then paused for 5 minutes to ensure all connections were secure and no abnormalities were observed. The unloading phase followed at the same loading rate until the jack load reading returned to its starting position. After a 5-minute rest, the load was reapplied to the specimen at the same loading rate until one of the following two criteria was met: either at least a 30% strength degradation was observed, or the maximum actuator stroke length was reached, at which point the test was stopped.

2.2 Specimen design and test matrix

The test program includes six double-storey CFSSW specimens with varying built-up uplift and flooring configurations and sheathing thicknesses.. Each shear panel, with dimensions 2400 mm (high) and 1200 m (wide), is composed of the following components and specimen assembly drawings are illustrated in Fig. 6:

- Stud member: Cold-rolled G450 Lysaght Cee sections, C15024, with depth (d) of 152 mm, flange width (w) of 63 mm, and lip width (l) of 18.5 mm, as per Fig. 5 (a).
- Track member: GALVABOND G2 steel sheet of 2.4 mm thickness, press-braked into 168 mm (d) × 68 mm (w) C-shaped channel, as Fig. 5 (b).
- Rim track member: GALVABOND G2 steel sheet of 2.4 mm thickness, cut to size and pressed to form a 304 mm (d) × 73 mm (w) C-shaped channel, as per Fig. 5 (b).
- Sheathing: GALVABOND G2 steel sheet of 0.55 mm and 1.10 mm mill thicknesses, cut to size of 1220 mm by 2400 mm.
- Sheathing-to-frame fastener: G8.8 #10 pan head screw, spaced at 75 mm and with edge distances of 37.5mm and 47.5 mm in the vertical and horizontal directions respectively.
- Built-up fastener: G8.8 #10 hex head screws with 150mm spacing and 75mm distance to the edges at both ends. Fasteners are positioned at the centreline of the lips of one component channel section, as illustrated in Fig. 5 (c).

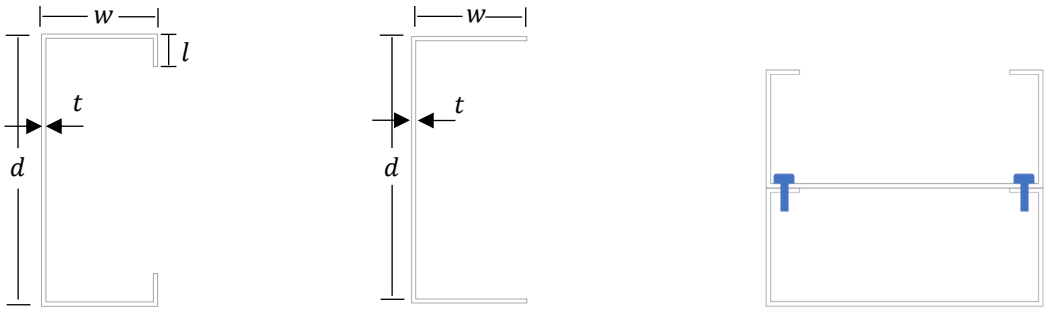

(a) Stud Cee section (b) Track and rim track section (c) 2C built-up connection

Fig. 5: Specimen component drawings

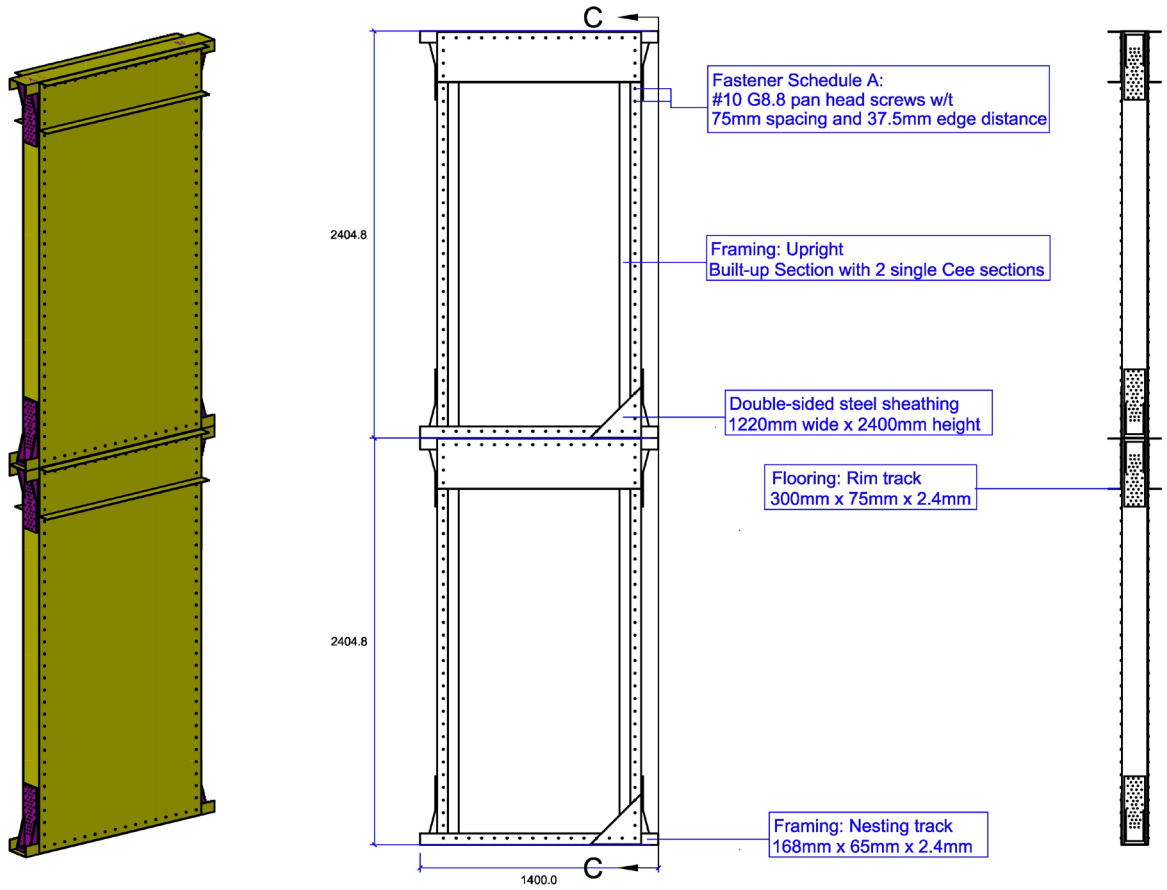

(a) 3D drawing (b) 2D elevation view (c) 2D side view

Fig. 6: 3D and side views drawings of specimen BU2C-10D-1-M-1

The experimental test matrix is outlined in Table 1. The specimen ID nomenclature defines the key parameters used in the table, including the built-up configurations (B_{config}), fastener schedule (F), sheathing thickness (t_{sheath}), and load type (L). All specimens have consistent single panel dimensions of 2400 mm in height and 1200 mm in width, and an overall specimen height of 4800mm. Stud types include built-up sections comprised of 2 single sections ($BU2C$) and equally spaced stud (ES) arrangements. Fastener schedules (F) are specified as $10S$ or $10D$, with reference to the screw size (gauge 10) and perimeter fastener schedule, where S refers to a single line of fasteners connecting the sheathing to the uprights and D indicates double lines. Sheathing thicknesses are denoted as 1 or 2, indicating base metal thicknesses of 0.55 mm and 1.10 mm respectively. The load type is also included in the nomenclature as a potential variable in the future when cyclic loading will be introduced. Specimen BU2C-10S-1-M-1 is considered a dummy test to understand the common failure modes for a double-storey shear wall system. It is also used to refine specimen design during the initial stage, including instrumentations, loading mechanism, and hold-down connections.

Material properties for stud, track, rim track and sheathing components adopted in this test series are determined from standard flat tensile coupon tests and summarised in Table 2. Key properties including Young's Modulus (E), yield strength (F_y), and tensile strength (F_u) are calculated according to the proposed data processing method by Huang and Young (2014).

Table 1: Test matrix for double storey CFSSW test program

Test No.	Specimen ID	B_{config}	F	t_{sheath} (mm)	L	Repetition
1	BU2C-10S-1-M-1	BU2C	10S	0.55	M	1
2	BU2C-10S-1-M-2	BU2C	10S	0.55	M	2
3	BU2C-10S-1-M-3	BU2C	10S	0.55	M	3
4	ES-10S-1-M-1	ES	10S	0.55	M	1
5	BU2C-10D-2-M-1	BU2C	10D	1.1	M	1
6	BU2C-10D-1-M-1	BU2C	10D	0.55	M	1

Table 2: Material property matrix for test components

Specimen Name	t (mm)	b (mm)	Steel Grade	E (GPa)	F_y (MPa)	F_u (MPa)
STUD	2.39	12.5	G450	210.28	522.68	554.61
TRACK	2.4	12.5	G450	213.94	513.84	539.26
w**STH**_1.10	1.1	12.2	G300	197.66	272.14	331.54
STH_0.55	0.55	12.25	G300	202.26	322.72	348.51

3. Test observations and results

3.1 Summary of experimental results

For all specimens, due to the small thickness of the sheathing, elastic buckling of the sheets initiated at a very early stage of the test. For the conducted tests, measurements of displacement and rotation were collected to capture the overall behaviour of the specimens. A summary table of the test results was generated based on the raw instrumentation measurements, as shown in Table 3. The table outlines the shear stiffness (K_e), shear capacity (F_u), maximum story drift at the storey levels (denoted as d_{F1}, d_{F2}), in-plane panel rotation (θ_1, θ_2), panel uplift at both levels (U_{F1-T}, U_{F2-T}, and U_{F2-C}) on the tension (T) and compression (C) sides, as well as between-floor separation (δ_{btw}). Some of these responses are schematically illustrated in Fig. 10, including lateral displacements ($\delta_{x,1}$ and $\delta_{x,2}$), uplift displacements (U_{F1-T}, U_{F2-T}, and U_{F2-C}), rotations (θ_1 and θ_2), and between-floor separation (δ_{btw}). Shear stiffness is calculated as the slope of the initial load displacement curve within the initial linear stage up t a load of 40% of the ultimate load. The lateral (x-axis) displacements are assumed to be positive in the direction of the applied load, while positive vertical (y-axis) displacements represent uplift at the measured location. Positive in-plane panel rotation at each floor is denoted as the counterclockwise direction from positive y to positive x. Storey drift is calculated as Eq. 1, based on storey height and the lateral displacement developed at the floor of interest. Graphical indication of key responses is shown in Fig. 7.

$$d_{Fn} = \frac{\delta_{x,n} - \delta_{x,n-1}}{storey\ height} \times 100\% \text{ where, } n = \text{shear wall floor level} \quad \text{Eq. 1}$$

Sheathing buckling patterns for all specimens are presented in Fig. 8, and detailed discussions can be found in the following Sections 3.2, 3.3 and 3.4.

Table 3: Experimental results for cold-formed steel shear wall specimens

Specimen ID	K_e (kN/mm)	F_u (kN)	δ_{btw} (mm)	d_{F1}	d_{F2}	θ_1 (rad)	θ_2 (rad)	$U_{F1\text{-}T}$ (mm)	$U_{F2\text{-}T}$ (mm)	$U_{F2\text{-}C}$ (mm)
BU2C-10S-1-M-2	0.67	49.56	1.52	1.76%	2.09%	17.56E-03	3.29E-03	2.99	6.16	-10.21
BU2C-10S-1-M-3	0.58	53.24	1.14	2.61%	2.15%	26.11E-03	-4.59E-03	3.74	5.83	-8.45
ES-10S-1-M-1	0.67	54.72	0.22	2.50%	2.13%	24.97E-03	-3.65E-03	3.44	8.41	-9.46
BU2C-10D-2-M-1	0.88	107.17	1.25	3.68%	3.88%	36.76E-03	1.98E-03	16.34	21.35	-15.29
BU2C-10D-1-M-1	0.83	64.96	3.59	2.18%	2.61%	21.75E-03	4.30E-03	4.35	7.26	-11.91

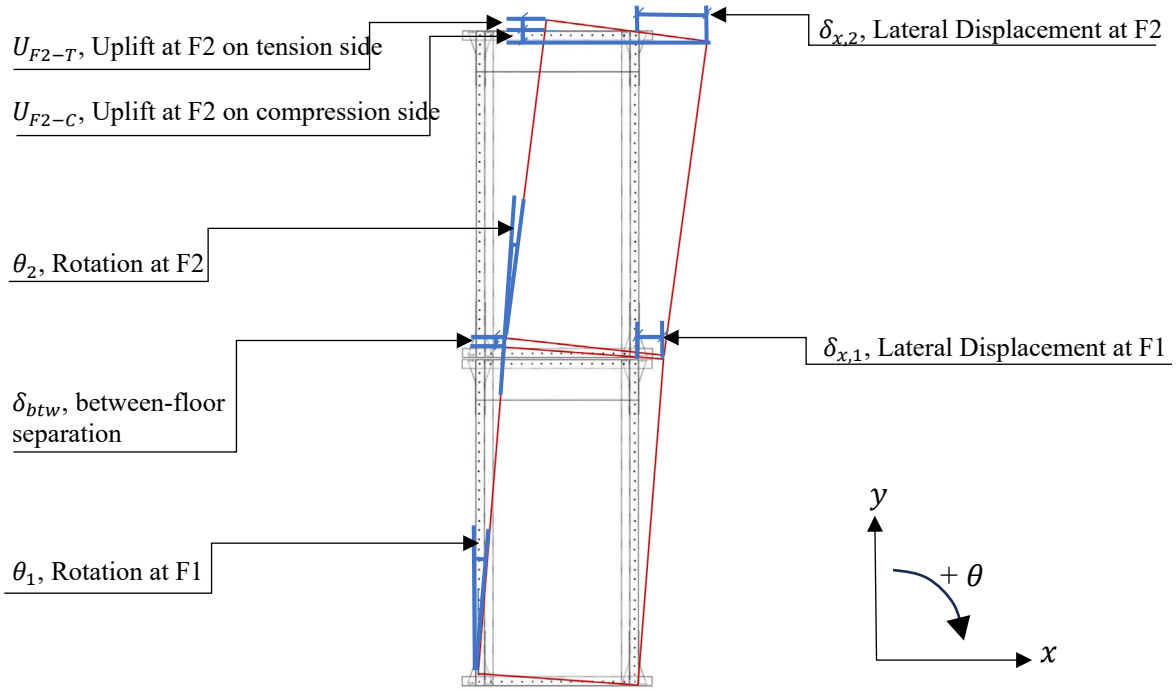

Fig. 7: Graphical representation of parameters and responses measured in CFSSW tests

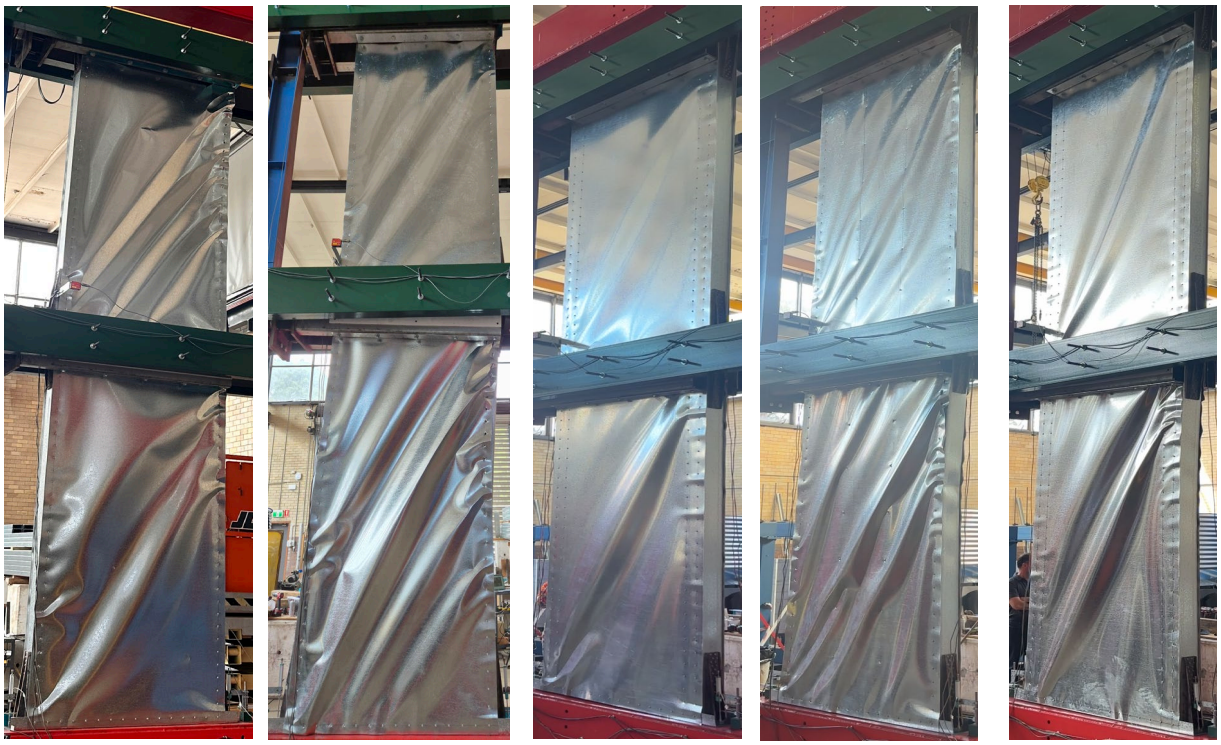

(a) BU2C-10S-1-M-2 (b) BU2C-10S-1-M-3 (c) ES-10S-1-M-1 (d) BU2C-10D-2-M-1 (f) BU2C-10D-1-M-1

Fig. 8: Sheathing buckling pattern of each specimen

3.2 Effects of floor configuration

Fig. 8 (a) illustrates the sheet buckling pattern at failure for specimen BU2C-10S-1-M-2. Extensive plastic deformation is evident in the top panel, which is significantly more pronounced compared to the bottom panel. By analysing the deformed shape of the panel frames, the observations confirm that failure occurred predominantly at the second level. Focusing on the failure region, as shown in Fig. 9 (a), the sheathing has completely detached from the framing due to the failure of screws within the sheathing tension fields. To identify the dominant fastener failure modes, the specimen was disassembled. Rim tracks were removed from the panel, and perimeter fasteners were unscrewed from the frame for inspection. As shown in Fig. 9 (b), sheet bearing and tear out failures were identified at the top tension band corner of the upper panel. Observation of the fastener failure modes revealed that shear and tension failure were the dominant modes for this test. Further examination also revealed significant flexural buckling deformations of the web of the top track of the upper panel, as visualised in Fig. 9 (c). This localised deformation, caused by the downward force applied by the hold-down bracket, underscores the stress concentration and failure mechanism in the upper framing component. It suggests that to accurately capture the failure of an inter-storey panel, modification of the floor configuration at the top of the specimen is required. To this end, another assembly was designed.

(a): Separation of sheathing from the frame on both sides

(b): Bearing and tear-out failures of the sheathing

(c): Web deformations of the top track

Fig. 9: Failure mechanism of specimen BU2C-10S-1-M-2, at upper panel

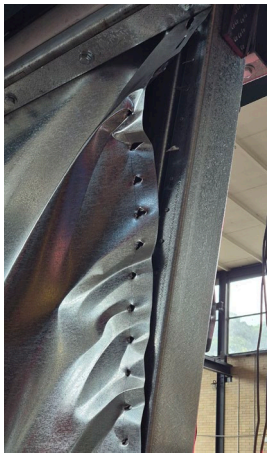

Fig. 10 Separation of sheathing at lower panel for specimen BU2C-10S-1-M-3

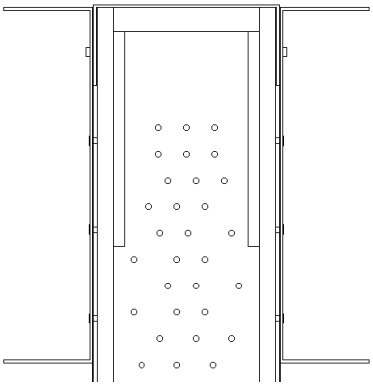

(a) specimen BU2C-10S-A-M-2

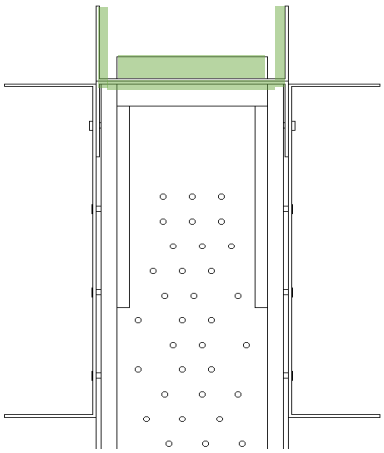

(b) specimen BU2C-10S-A-M-3

Fig. 11: Floor configuration variations adopted in the test program

The top floor assembly of specimen BU2C-10S-1-M-2 was designed as shown in Fig. 11 (a). For specimen BU2C-10S-1-M-3, an additional track was installed at the top, along with four 65 mm × 60 mm × 20 mm steel plates, as shown in Fig. 11 (b). These additional components were included to replicate the stiffness and boundary conditions provided by the shear panel one level above in a real building structure. At the failure stage of the test, as depicted in Fig. 8 (b) and Fig. 10, substantial buckling was observed in the lower panel, highlighting a shift in the failure mechanism to this panel.

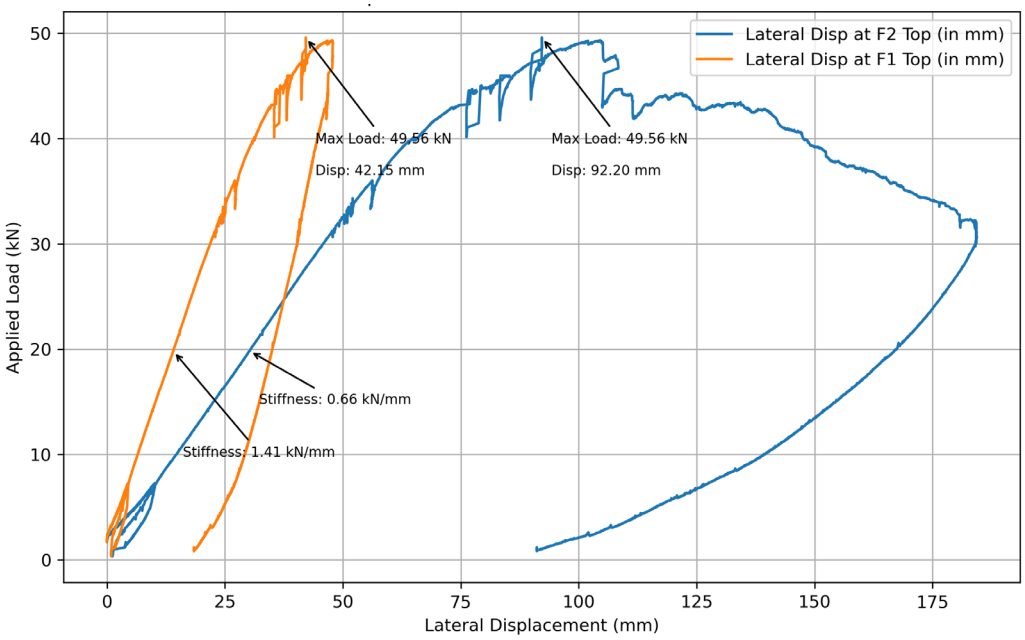

(a): Specimen BU2C-10S-1-M-2

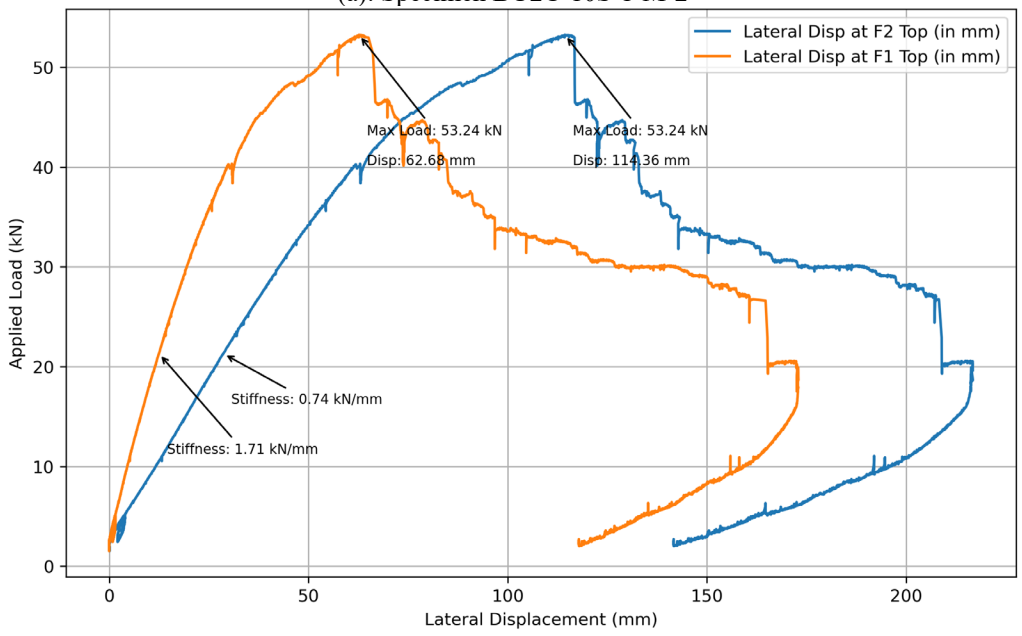

(b): Specimen BU2C-10S-1-M-3

Fig. 12: Applied load vs. lateral displacement recorded at the top of floors level 1 and 2

The load-displacement curves for specimens BU2C-10S-1-M-2 and BU2C-10S-1-M-3 are presented in Fig. 12(a) and Fig. 12(b), respectively. Specimen BU2C-10S-1-M-2 exhibited a shear capacity, F_u, of 49.6 kN with associated lateral displacements, $\delta_{x,1}$ and $\delta_{x,2}$, of 42.4 mm and 92.2 mm, respectively. A comparison of these curves reveals distinct behavioural differences between the two specimens. For BU2C-10S-1-M-3, the load-displacement curves for both levels followed a similar trend throughout the loading process. In contrast, for BU2C-10S-1-M-2, the curves diverged after the ultimate load was achieved as failure localised in the upper panel. These

displacement measurements reflect the observed shift in the failure mode from the second floor to the first floor, caused by the additional track and packers at the top of the upper panel. This failure mode of BU2C-10S-1-M-3 aligns with the predicted failure mode in real mid-rise cold-formed steel structures, where the most larger shear force is transferred to the bottom panel, causing it to fail first. Based on these findings, the design of all subsequent test specimens was revised to integrate the additional components, namely the track and the bottom plates of hold-down brackets at the top of the upper panel.

3.3 Effect of built-up section

In this section, three specimens — BU2C-10S-1-M-3, ES-10S-1-M-1, and BU2C-10D-1-M-1— are compared to better understand the role of built-up sections in CFSSWs. The comparison between tests BU2C-10S-1-M-3 and ES-10S-1-M-1 focused on the effect of the upright configuration, with the only controlled variable between the tests being the framing arrangement. In specimen BU2C-10S-1-M-3, each upright consisted of two single sections connected front-to-back to form a built-up section, whereas in specimen ES-10S-1-M-1, four single equally spaced uprights were used with two placed in the middle of the panel. Despite the similar shear capacities, distinct failure modes were identified. Fig. 8 (c) illustrates the sheathing buckling patterns and deformed frame configurations for specimen BU2C-10S-1-M-3.

For specimen ES-10S-1-M-1, the loss of structural integrity was attributed to a combination of fastener pull-through failures (Fig. 13 (a)) and the vertical framing member failing under combined axial compression and bending (as captured in Fig. 8 (d)). Hence, all three essential components of the panels, viz. uprights, sheathing and fasteners, reached their ultimate capacity and contributed to the failure. In comparison, as discussed in Section 3.2, the failure mechanism for BU2C-10S-1-M-3 was dominated by only the failure of the sheath-to-frame connections. More specifically, failure was initiated by the shear and tension fracture of the fasteners, followed by sheathing tear-out and pull-through. While small local buckling deformations of the web of the outer upright occurred on the compression side, the framing members remained within the elastic range These differences suggest that the use of built-up sections allowed the sheathing to achieve its full capacity, while the framing members retained additional axial and flexural strength reserves. This finding demonstrates that the adoption of built-up sections provides an opportunity to enhance the strength and optimise the performance of CFSSWs.

To further investigate the observed behaviour, double lines of fasteners were incorporated into specimen BU2C-10D-1-M-1. As shown in Fig. 13 (b), the failure mechanism of this specimen was primarily characterised by tearing and pull-through failure of the sheathing, while the built-up sections remained within the elastic region at the ultimate load. Notably, the adoption of double lines of fasteners prevented any instances of perimeter fastener shear or tension failure. The load-displacement curves (as illustrated in Fig. 14) indicate an increase in shear stiffness of the specimens. Specifically, the shear stiffness improves from 0.65 kN/mm for specimen ES-10S-1-M-1 to 0.74 kN/mm for BU2C-10S-1-M-3, and further to 0.83 kN/mm for BU2C-10D-1-M-1. . In terms of strength, there is no significant enhancement in the overall shear capacity between specimens ES-10S-1-M-1 (54.7 kN) and BU2C-10S-1-M-3 (53.2 kN). However, the load displacement curve for BU2C-10D-1-M-1 reveals an increased shear capacity of 65.0 kN, indicating the effectiveness of the double fastener arrangement in improving the structural performance.

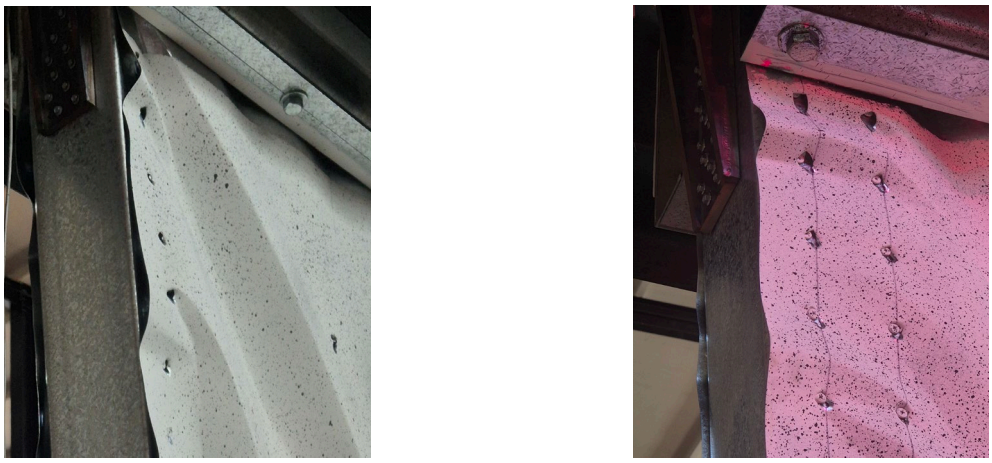

(a) specimen ES-10S-1-M-1 (b) specimen BU2C-10D-1-M-1

Fig. 13: Sheet separation at F1 panel top tension field

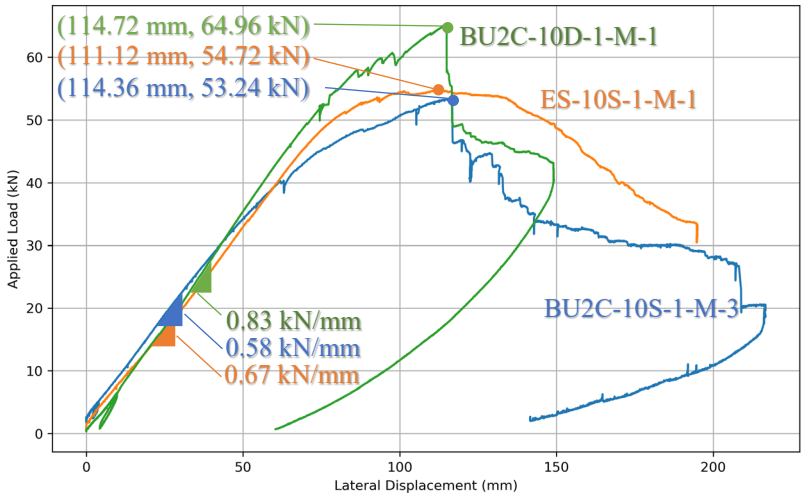

Fig. 14: Lateral displacement recorded at the top of floor level 2 for specimen ES-10S-1-M-1, BU2C-10S-1-M-3, and BU2C-10D-1-M-1

These results emphasize that although the inclusion of double fasteners improves both shear stiffness and shear capacity, the failure mechanism continues to be governed primarily by the sheathing response. The built-up sections, however, remain within their elastic range. This underscores the potential for optimizing fastener arrangements to enhance structural performance while mitigating critical failure modes. Therefore, an increase in the sheathing thickness is deemed necessary, improving the critical component of the panels.

3.4 Effect of sheathing thickness

From the three tests discussed in the previous section, it is evident that stronger sheathing is essential to better utilise the strength of the built-up uprights and achieve improved shear resistance. For test specimen BU2C-10D-2-M-1, the thickness of the sheathing was doubled from 0.55 mm to 1.1 mm. As shown in the load-displacement plots in Fig. 15, both the initial shear stiffness and especially the shear capacity are enhanced, with increases of 6% and 65%,

respectively, achieved solely by doubling the sheathing thickness. Furthermore, an examination of the buckling behaviour of the sheathing in specimen BU2C-10D-2-M-1, as shown in Fig. 8 (e), reveals significantly reduced out-of-plane displacement at the ultimate load compared to specimens with thinner sheathing.

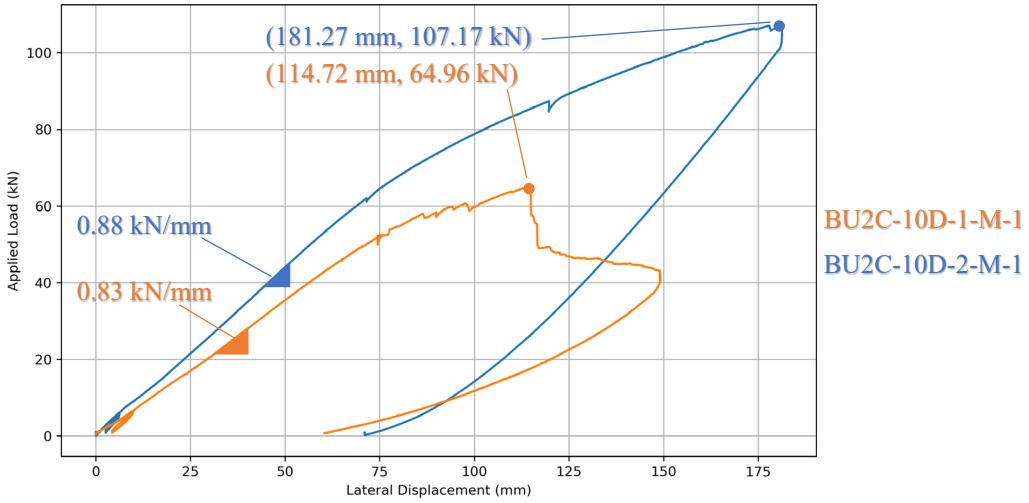

Fig. 15: Load displacement curves for specimens with 0.55 mm and 1.1 mm sheathing thicknesses.

The test was terminated when the actuator reached its maximum stroke limit. At the termination point, minor tearing damage was observed at the fastener near the top corner of the bottom panel, but no catastrophic failure of the specimen occurred. The framing members exhibited only minor local buckling of the web, indicating that the built-up sections retained significant residual capacity despite the increased demands placed on the system. When combined with the findings in Section 3.3, compelling evidence highlights the advantages of utilising built-up uprights in CFSSW systems. The more robust framing members enable the use of thicker sheathing, which is critical for improving shear resistance without increasing overall wall thickness. This demonstrates the potential of built-up uprights to enhance structural performance and material efficiency.

4. Conclusions

This study investigates the performance of CFSSWs through a series of double-storey shear wall tests designed to replicate mid-rise building conditions. The experimental program includes six specimens with varying built-up upright and floor configurations, sheathing thicknesses and fastener schedules. The tests are conducted on a self-reactive frame under monotonic loading, with load applied to flooring components through slotted scissor joints. Key performance metrics such as shear stiffness, capacity, drift, and uplift are analysed. The results demonstrates that built-up uprights significantly improved system stiffness and stability, enabling the sheathing to reach full tension capacity while maintaining the integrity of framing members. Doubling the sheathing thickness increases the shear capacity by 65% and stiffness by 6%, while the reduced out-of-plane displacements at the ultimate load highlights improved lateral stability. By combining single channels into built-up sections, both higher bending and axial capacity of the uprights are achieved, allowing system optimisation and enabling the effective utilisation of stronger framing members and connectors. Incorporating double fastener lines further enhanced the load transfer mechanism, increasing the shear capacity by 22% from 53.2kN for single fastener lines to 65.0 kN.

These findings highlight the importance of balancing the strengths of the critical components when optimising CFSSWs for mid-rise structures. Currently adopted shear wall systems with single sections are unable to fully harness the capacity of the sheathing. The incorporation of built-up sections successfully addresses this limitation, allowing for better utilisation of the sheathing's strength. This is also achieved by simultaneously increasing the number of perimeter connectors. The test results provide valuable data for validating computational models and advancing design guidelines for more efficient and resilient shear wall systems for mid-rise CFS structures. In the future, further tests will be conducted as series two of the test program and is intended to have a focus on different built-up upright sizes with matching optimised sheathing thickness and fastener arrangement.

Acknowledgments
The research described in this paper is supported by the Australian Research Council (ARC) Discovery Project DP220103573.

References

American Society for Testing and Materials. 1998. "Standard Practice for Static Load Test for Shear Resistance of Framed Walls for Buildings." *ASTM E 564-95, Annual Book of Standards* 4.

Boudreault, Félix-Antoine. 2005. "Seismic Analysis of Steel Frame Wood Panel Shear Walls."

Brière, Vincent. 2018. Higher Capacity Cold-Formed Steel Sheathed and Framed Shear Walls for Mid-Rise Buildings: Part 2. Master's Thesis, McGill University (Canada).

Driver, Robert G, Geoffrey L Kulak, DJ Laurie Kennedy, and Alaa E Elwi. 1998. "Cyclic Test of Four-Story Steel Plate Shear Wall." *Journal of Structural Engineering* 124(2): 112–20.

Huang, Yuner, and Ben Young. 2014. "The Art of Coupon Tests." *Journal of Constructional Steel Research* 96: 159–75.

Li, Chao-Hsien, Keh-Chyuan Tsai, Chih-Han Lin, and Pei-Ching Chen. 2010. "Cyclic Tests of Four Two-story Narrow Steel Plate Shear Walls. Part 2: Experimental Results and Design Implications." *Earthquake Engineering & Structural Dynamics* 39(7): 801–26.

Mori, Kyohei, Kyohei Murakami, Masanobu Sakashita, Susumu Kono, and Hitoshi Tanaka. 2008. "Seismic Performance Of Multi-Story Shearwall With An Adjacent Frame Considering Uplift Of Foundation." *A A* 40: 25.

Peterman, K.D., N. Nakata, and B.W. Schafer. 2014. "Hysteretic Characterization of Cold-Formed Steel Stud-to-Sheathing Connections." *Journal of Constructional Steel Research* 101: 254–64. doi:10.1016/j.jcsr.2014.05.019.

Reynolds, Thomas, Robert Foster, Julie Bregulla, Wen-Shao Chang, Richard Harris, and Michael Ramage. 2017. "Lateral-Load Resistance of Cross-Laminated Timber Shear Walls." *Journal of Structural Engineering* 143(12): 06017006.

Santos, Veronica. 2018. Higher Capacity Cold-Formed Steel Sheathed and Framed Shear Walls for Mid-Rise Buildings: Part 1. Master's Thesis, McGill University (Canada).

Serrette, Reynaud, Jose Encalada, Georgi Hall, Brandon Matchen, Hoang Nguyen, Alexander Williams, and Light Gauge Steel Research Group. 1997. “Additional Shear Wall Values for Light Weight Steel Framing (Draft).”

Serrette, Reynaud, I Lam, H Qi, H Hernandez, and A Toback. 2006. “Cold-Formed Steel Frame Shear Walls Utilizing Structural Adhesives.” *Journal of Structural Engineering* 132(4): 591–99.

Shahnewaz, Md, Carla Dickof, and Thomas Tannert. 2021. “Seismic Behavior of Balloon Frame CLT Shear Walls with Different Ledgers.” *Journal of Structural Engineering* 147(9): 04021137.

Shamim, Iman, Jamin DaBreo, and Colin A. Rogers. 2013. “Dynamic Testing of Single- and Double-Story Steel-Sheathed Cold-Formed Steel-Framed Shear Walls.” *Journal of Structural Engineering* 139(5): 807–17.

Singh, A, X Wang, Z Zhang, F Derveni, H Castaneda, KD Peterman, BW Schafer, and TC Hutchinson. 2020. “Lateral Response of Cold-Formed Steel Framed Steel Sheathed In-Line Wall Systems Detailed for Mid-Rise Build.”

Wang, Xingxing, and Jihong Ye. 2016. “Cyclic Testing of Two- and Three-Story CFS Shear-Walls with Reinforced End Studs.” *Journal of Constructional Steel Research* 121: 13–28.

Yu, Cheng. 2010. “Shear Resistance of Cold-Formed Steel Framed Shear Walls with 0.686 Mm, 0.762 Mm, and 0.838 Mm Steel Sheet Sheathing.” *Engineering Structures* 32(6): 1522–29.

Zhang, Zhidong, Mohammed M Eladly, Colin A Rogers, and Benjamin W Schafer. 2024. “Cold-Formed Steel Framed Shear Wall Test Database.” *Earthquake Spectra* 40(1): 871–84.